Planetary and Space Science 98 (2014) 120–127

Contents lists available at ScienceDirect

Planetary and Space Science

journal homepage: www.elsevier.com/locate/pss

Impact induced erosion of hot and dense atmospheres

Valery Shuvalov [a], Ekkehard Kührt [b], Detlef de Niem [b,*], Kai Wünnemann [c]

[a] Institute of Geospheres Dynamics, Russian Academy of Sciences, Leninskii Prospekt 38-1, 119334 Moscow, Russia
[b] German Aerospace Center, Institute of Planetary Research, Rutherfordstraße 2, D-12489 Berlin, Germany
[c] Museum für Naturkunde, Invalidenstraße 43, D-10115 Berlin, Germany

ARTICLE INFO

Article history:
Received 29 January 2013
Received in revised form
9 August 2013
Accepted 23 August 2013
Available online 31 August 2013

Keywords:
Meteorite impact
Atmospheric evolution
Earth

ABSTRACT

Previous investigations of impact-induced atmospheric erosion considered mainly crater-forming impacts. Simple estimates show that in dense primary planetary atmospheres, considerable erosion could be induced by aerial bursts resulting from impacts of 1–10 km sized projectiles. Numerical simulations of cometary and asteroidal impacts (striking unmodified and crater-forming, impacting as fragmented meteorites, or causing aerial bursts) into dense (200 bar) atmospheres of different temperatures have been performed to obtain the amount of atmospheric erosion. The results have been approximated by simple analytical formulae.

1. Introduction

The evolution of Earth's atmosphere is characterized by source and loss processes. Atmospheres may have evolved by gravitational attraction from the solar nebula, whereas the Earth's atmosphere more likely is a product of volcanic degassing from the mantle and evaporation of volatiles during impact of comets and hydrous asteroids. The growth of atmospheres is counteracted by escape processes primarily due to hypervelocity impacts. The idea of impact-induced planetary atmospheric erosion has been suggested by Cameron (1983). It is based on the assumption that a considerable mass of shock-heated and upwards-accelerated atmospheric gas can reach velocities exceeding $u_{esc}=11.2$ km/s (i.e., escape velocity for the Earth) and can be ejected to space.

Quantitative estimates of this mechanism based on different assumptions have been proposed by Vickery and Melosh (1990), Newman et al. (1999), and Shuvalov and Artemieva (2002). Simple approximations treated impacts like surface explosions. The most advanced models (Svetsov, 2007; Shuvalov, 2009) consider the cratering flow induced by impacts of spherical or cylindrical asteroids and comets. de Niem et al. (2012) coupled previously suggested parameterizations of source and loss processes with an estimated impactor flux in a stochastic model to quantify atmospheric evolution; however, they pointed out that a comprehensive description of the impact-induced loss mechanism is lacking. Although Shuvalov (2009) has taken the effects of impact angle and of a wake created during the flight of the projectile through the atmosphere into account, the possible disruption and/or deceleration of the projectile during its passage through the atmosphere at different impact angles has not been considered yet.

Nemchinov and Shuvalov (2003) and Svetsov (2007) have shown that vertical impacts of comets 100–300 m in diameter, which would disrupt and decelerate considerably in the atmosphere, cause significant erosion of the Earth's atmosphere. In such a case the ratio of escaping mass relative to the impactor mass reaches up to a few tens of percent. They concluded that such objects could significantly influence the evolution of the atmosphere. However, the existence of such small comets and their number are still being questioned. At least, small comets are not considered to be a major type of Earth's impactors (Kuzmitcheva and Ivanov, 2008). Alternatively to an intense bombardment and efficient erosion of the atmosphere by small bodies, much larger projectiles may be decelerated and fragment during their entry if the atmosphere has been much denser, probably dozens of bars. Such conditions may have been realistic for the primary Earth's atmosphere (Zahnle et al., 2007) that is assumed to have been considerably more massive (up to 200 bar) and hotter (above 1000 K) than the modern one. In such an atmosphere comets and even asteroids a few kilometers in diameter could be totally disrupted and decelerated and may have transferred their energy almost completely to the air producing aerial bursts (Wasson and Boslough, 2000). This process, in turn, could result in strong impact induced atmospheric erosion.

De Niem et al. (2012) applied a Monte Carlo method and found that after a heavy bombardment period the feeding of atmospheres is the dominating process in competition of erosion and retention of atmophile constituents of the impactors for a wide

* Corresponding author. Tel.: +49 3067055 316; fax: +49 3067055 303.
E-mail addresses: shuvalov@idg.chph.ras.ru (V. Shuvalov), ekkehard.kuehrt@dlr.de (E. Kührt), detlef.deniem@dlr.de (D. de Niem), kai.wuennemann@mfn-berlin.de (K. Wünnemann).

0032-0633/$ - see front matter © 2013 Elsevier Ltd. All rights reserved.
http://dx.doi.org/10.1016/j.pss.2013.08.018

range of input parameters when starting with thin or moderate atmospheric densities. In order to extend the initial conditions for such an approach towards the more realistic assumption of a dense primary atmosphere on Earth we have conducted a new parametric study on impact-induced atmospheric erosion based on a previous approach by Shuvalov (2009).

The purpose of this study is to simulate cometary and asteroidal impacts into dense and hot atmospheres and to estimate atmospheric erosion induced by aerial bursts produced by projectiles disintegrating and decelerating above the Earth's surface. Such impactors do not produce craters and are therefore not manifest in the crater record. A concomitant goal is to study the influence of atmospheric density and temperature (given by atmospheric scale height) on projectile evolution during the entry. The results can be used to evaluate the evolution of dense atmospheres in a period of heavy bombardement.

Numerical simulations (Shuvalov, 2009) have shown that angle-averaged data on atmospheric erosion correlate well with the results for an impact angle of 45° (the most probable angle of incidence). For this reason we consider only 45° oblique impacts in this study.

2. Numerical model

The 3D numerical model described in Shuvalov (2009) cannot directly be applied for modeling impacts when projectiles experience strong fragmentation and deceleration during their atmospheric traversal. Numerical modeling of atmospheric entry in the modern atmosphere (Shuvalov and Trubetskaya, 2007) has shown that significant deformation, fragmentation, and deceleration of projectiles with sizes considerably smaller than the atmospheric scale height occur at a distance of about 100 projectile sizes. At the same time the simulation of projectile deformation and fragmentation requires rather high spatial resolution (more than 40 cells per projectile diameter). To account for both, a sufficiently large computational domain and high resolution, one would need an unrealistically large numerical mesh (1000–10,000 cells in one direction) to address the problem in a 3D geometry.

To overcome this problem we employed a two-step model approach. In the first step we use a 2D cylindrically symmetric grid (Shuvalov and Trubetskaya, 2007) to describe the processes of atmospheric entry, projectile deformation, fragmentation and deceleration. The 2D models allows for a very high-resolution grid of 40 cells per projectile radius along the central region. The cell size increases at long distances behind the projectile where the flow is almost cylindrical, all gradients along the trajectory are small, and high resolution is not needed. The impact angle $\alpha=45^\circ$ is taken into account by decreasing gravity by a factor of $\sin(\alpha)$ and increasing atmospheric scale height by its inverse. This approach was previously used for modeling Tunguska and Schoemaker-Levy9 comet impacts (Shuvalov and Trubetskaya, 2007; Shuvalov et al., 1999). The 2D approximation can be used until the wake radius is less than the atmospheric scale height H. In the second step the output from the 2D model is taken as an initial data set for the 3D model. To solve the 3D problem we use the same approach as described in Shuvalov (2009). The falling body is assumed to be quasi-liquid (with zero strength). This approximation is suitable for cases of rather large bodies that are destroyed before there is noticeable deformation (Svetsov et al., 1995).

This two-step model cannot be used when the projectile size is comparable with the atmospheric scale height, because in this case 3D effects become significant from the very beginning of projectile entry. However, the results of numerical simulations show that such large projectiles do not experience strong deformation and deceleration, and the 3D model can be used for modeling such impacts ab initio.

We considered impacts into a dense atmosphere with mass exceeding that of the modern terrestrial atmosphere by a factor of 200. Consequently the pressure near the surface equals 200 bar. The atmosphere was considered to be about 5 times warmer (1500 K near the surface) than the modern one and had a characteristic scale height H of about 40 km. For comparison some runs were carried out with a cold (resembling the modern) atmosphere with $H\approx 8$ km.

Tabulated data generated by the ANEOS equation of state (Thompson and Lauson, 1972) using input parameters from Pierazzo et al. (1997) for dunite and granite were applied to describe the thermodynamic behavior of stony projectiles and target material. We used Tillotson's equation of state (Tillotson, 1962) to describe cometary material and a tabular equation of state (Kuznetsov, 1965) for the atmospheric gas. To understand a possible influence of atmospheric composition on the impact process we performed a few additional runs with an atmosphere of the same mass and scale height but assumed a perfect gas EOS with a specific heat ratio of 1.4.

3. Results

3.1. Atmospheric entry

Small (about 1 m sized) meteorites usually experience fragmentation at altitudes of about 40–50 km where aerodynamic loading is about 10^7 dyn/cm^2 (Svetsov et al., 1995). The probability of large defects grows with meteorite size, and the ultimate strength decreases (Tsvetkov and Skripnik, 1991). Therefore large bodies experience fracture at higher altitudes. An increase of atmospheric density at the surface further increases the altitude of fracturing. However, aerodynamic loading at high altitudes is too small to separate fragments of a large meteorite and it continues to move as a single body consisting of closely packed fragments surrounded by a single shock wave. The main deformation starts at lower altitudes where the body is completely fractured and can be treated as liquid-like. A more comprehensive treatment of material strength to study fracturing at high altitudes would barely change the process of deformation at low altitudes. Thus we considered deformation, fragmentation, and deceleration of liquid-like projectiles.

Fig. 1 illustrates sequential stages of the atmospheric entry of a 3-km-diameter comet entering the Earth atmosphere with a velocity of 50 km/s at an angle of 45°. The comet is assumed to consist of pure water ice with a density of 1000 kg/m^3, for asteroids a density of 3300 kg/m^3 has been chosen.

The comet begins to deform at an altitude of about 200 km due to development of Rayleigh–Taylor and Kelvin–Helmholtz instabilities. At higher aerodynamic loading, the comet is flattened and transforms into a pancake-like structure. The growth of instabilities results in fragmentation of the cometary pancake at an altitude of about 80 km. A jet consisting of shock-heated air and comet fragments is formed. The initial velocity of the jet (about 45 km/s) is only slightly lower than the entry velocity. Later the jet expands in radial direction and decelerates. At an altitude of about 60 km its velocity is halved. At this moment in time the 2D simulation is finished and the output is used as initial data set for the 3D model.

There is no qualitative difference between atmospheric entry of a comet and a stony asteroid. In both cases the aerodynamic loading is larger than projectile strength if we consider kilometre-sized impactors. The quantitative difference is caused mainly by the impactor density. Stony asteroids penetrate deeper into the

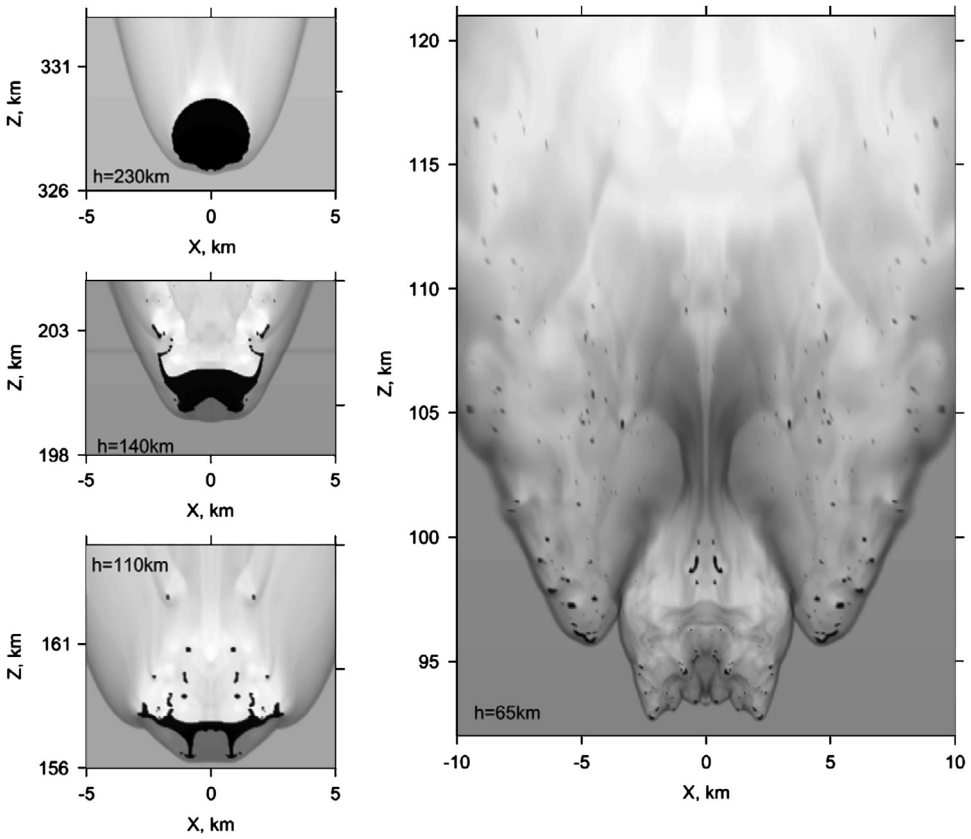

Fig. 1. Destruction of a 3-km diameter comet (run 3 in Table 1). The distributions of density (the darker–the denser) at different heights h are shown.

Table1
Parameters of atmospheric entry for different projectiles. N is the number of run, D the projectile diameter, V the entry velocity, ρ the projectile density, C/A distinguishes projectile type (comet or asteroid), H denotes atmospheric scale height, H_{fr} the altitude of fragmentation for disrupting projectiles, $H_{1/2}$ the altitude where projectile velocity is halved. U_{imp} is the impact velocity at the ground (for not severely decelerated projectiles). The values of H_{fr}, $H_{1/2}$, and U_{imp} are the results of numerical simulations. Asterisk marks cases with an ideal gas atmosphere.

N	D, km	V, km/s	ρ, g/cm^3	C/A	H, km	H_{fr}, km	$H_{1/2}$, km	U_{imp}, km/s
1	1.0	50	1.0	C	40	150	123	–
2	1.0	50	1.0	C	8	24	17	–
3	3.0	50	1.0	C	40	100	65	–
3*	3.0	50	1.0	C	40	101	63	–
4	3.0	50	1.0	C	8	10	4	22
5	3.0	30	1.0	C	40	97	60	–
6	3.0	20	1.0	C	40	98	67	–
7	10	50	1.0	C	40	10	–	37
8	10	50	1.0	C	8	–	–	41
9	10	30	1.0	C	40	20	–	20
10	10	70	1.0	C	40	15	–	54
11	30	50	1.0	C	40	–	–	46
12	100	50	1.0	C	40	–	–	50
13	1.0	20	3.3	A	40	125	88	–
14	1.0	20	3.3	A	8	18	12	–
15	3.0	20	3.3	A	40	60	35	–
16	3.0	30	3.3	A	40	63	40	–
17	3.0	20	3.3	A	8	4	–	11
18	10	20	3.3	A	40	–	–	17
19	30	20	3.3	A	40	–	–	20
20	100	20	3.3	A	40	–	–	20

atmosphere than comets of the same size and velocity. Simulation results for atmospheric entry of different projectile types at different conditions are summarized in Table 1.

Our numerical simulations show that the entry velocity very slightly influences the process of projectile deformation and disruption (see runs 3, 5 and 7, 9, 10 in Table 1). The altitudes of fragmentation and altitudes where projectile velocity is halved are rather close in runs with different pre-entry velocities but the same size and composition. This result correlates with simple estimates. The rate of projectile deformation u_d during the flight can be estimated from (Grigorian, 1979; Hills and Goda, 1993)

$$u_d = V(\rho_a/\rho_{pr})^{1/2}, \quad (1)$$

where V is the instantaneous velocity, ρ_a and ρ_{pr} are the densities of ambient air and impactor material respectively. Eq. (1) is analogous to that for growth of the largest length scale in the Rayleigh–Taylor instability (Svetsov et al., 1995). The deformation δ itself can be estimated as $\delta = u_d\tau$, where $\tau = S/V$ is the time of flight, S is the length of trajectory segment. Combining these relations one obtains

$$\delta = S(\rho_a/\rho_{pr})^{1/2}. \quad (2)$$

In conclusion, the deformation depends on trajectory length but not on impact velocity.

The process of deformation and fragmentation of a quasi-liquid meteoroid is accompanied by the development of Rayleigh–Taylor and Kelvin–Helmholtz hydrodynamic instabilities. These instabilities develop in a stochastic way; therefore, different results can be obtained even in different runs with the same initial data. This is the reason why the altitudes of fragmentation in runs 3, 5 and 7, 9, 10 slightly differ from each other. We define the altitude of fragmentation as that where the projectile transforms into several large (> 10% of the initial projectile) fragments.

The numerical results show that the projectiles decelerate faster and experience fragmentation at higher altitudes in warmer atmospheres (of the same mass but larger scale height and, consequently, lower surface density). A 1 km diameter comet decelerates (velocity halves) at an altitude of 123 km ($H_{1/2}/H \sim 3$) in the hot atmosphere and at an altitude of 17 km ($H_{1/2}/H \sim 2$) in the cold atmosphere. A 3-km-diameter comet decelerates at an altitude of 65 km ($H_{1/2}/H \sim 1.5$) in the hot atmosphere and at an altitude of 4 km ($H_{1/2}/H = 0.5$) in the cold atmosphere. The 'characteristic density of deceleration' equals $\rho_0 \exp(-H_{1/2}/H)$, where ρ_0 is the surface density. In a hotter atmosphere ρ_0 is smaller than in the cold one, and the relative altitude of deceleration $H_{1/2}/H$ is larger. Thus, one can see that in hotter atmospheres with the same mass the projectiles decelerate at smaller density. Moreover in hotter atmospheres the impactors experience a lower maximal atmospheric drag what could be of advantage for the delivery of organic material.

3.2. Atmospheric erosion

Fig. 2 shows the evolution of the disturbed region (wake) produced in the dense Earth atmosphere by impact of a 3-km-diameter comet. At the beginning of 3D simulations ($t=0$) the jet consisting of shock-heated air and projectile fragments is still moving downwards with a velocity of about 25 km/s. Approximately within 10 s the jet decelerates at an altitude of about 10 km above the surface. The structure looks very similar to simulations of the famous Tunguska event of 1908 (Vasilyev, 1998). The hydrostatic equilibrium is violated within the wake as high pressure and low density give rise to a large pressure gradient along the wake axis that cannot be balanced by gravity. As a result the hot air within the wake accelerates upwards along the wake axis (not vertically because of low drag within the rarefied wake). Deceleration of the jet consisting of hot air and projectile fragments results in the generation of a shock wave expanding along the wake in the upward direction (visible at $t=45$ s in Fig. 2). The shock wave further increases the pressure and upward directed flow along the wake. The wake itself slightly moves upwards in vertical direction.

This mechanism results in the formation of a jet (plume) directed upwards along the wake, that ejects air and projectile material to high altitudes (see Fig. 3). The fastest part of the plume may reach a velocity above the escape speed u_{esc} (11.2 km/s for the Earth) and lead to atmospheric erosion. At the impact of a 3-km-diameter comet the Earth's atmosphere loses an atmospheric mass of approximately $m_a = 0.4M$, where M is the projectile mass. Results of additional cases of atmospheric erosion are presented in Table 2.

The mass of escaping air m_a was determined as

$$m_a = \int f\rho_a u_z dxdydt, \quad (3)$$

where ρ_a is the atmospheric density, u and u_z are hydrodynamic velocity and its vertical component, dt is the time interval, $f=1$ if $u > u_{esc}$ and $u_z > 0$, otherwise $f=0$. The mass loss was integrated over a control surface at $z=800$ km in our models for $H=40$ km

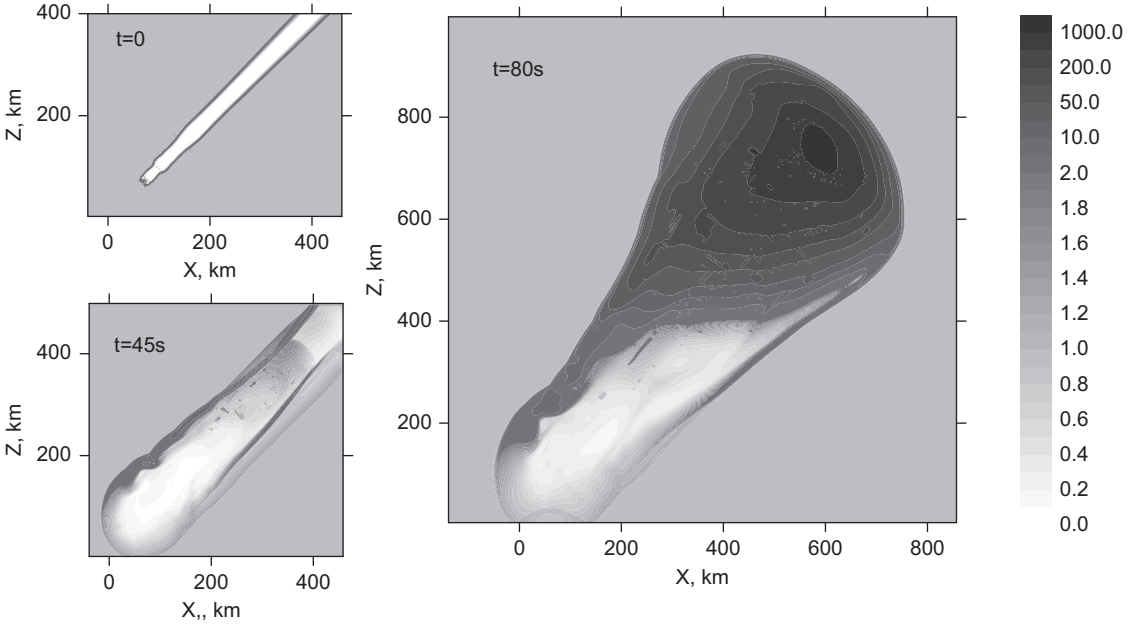

Fig. 2. Initial stage of plume formation after the impact of a 3 km diameter comet. Distributions of relative density $\rho/\rho_0(z)$ are shown, where $\rho_0(z)$ is equilibrium air density at an altitude z.

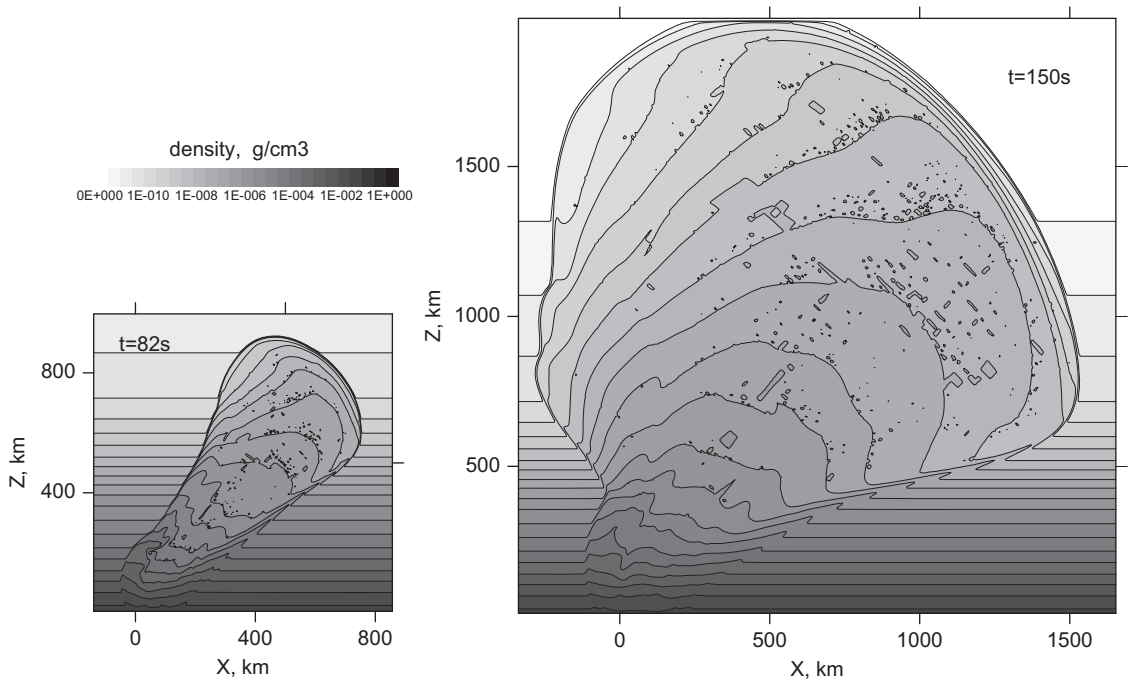

Fig. 3. Atmospheric plume produced by the impact of a 3-km-diameter comet. Distributions of density ρ are shown.

Table 2
Atmospheric erosion induced by impacts of different projectiles. *N* denotes the number of run, *D* the projectile diameter, *V* the entry velocity, ρ_{pr} the projectile density, C/A its type (comet or asteroid), *H* the atmospheric scale height. An asterisk marks cases with atmosphere modeled as ideal gas. Furthermore m_a/M and m_{pr}/M are escaping fractions of atmospheric and projectile masses in units of the meteorite mass (as obtained in numerical simulations), χ_a and ξ are dimensionless variables introduced by Shuvalov (2009).

N	*D*, km	*V*, km/s	ρ_{pr}, g/cm^3	C/A	*H*, km	m_a/M	χ_a	m_{pr}/M	Ξ
1	1.0	50	1.0	C	40	0.1	0.005	0	4.3e−3
2	1.0	50	1.0	C	8	0.6	0.03	0.01	0.11
3	3.0	50	1.0	C	40	0.4	0.02	0.005	0.12
4	3.0	50	1.0	C	8	0.04	0.002	0	2.9
5	3.0	30	1,0	C	40	0.03	0.0015	0	3.8e−2
6	3.0	20	1.0	C	40	< 1e−5	< 5e−7	0	1.4e−2
7	10	50	1.0	C	40	0.5	0.025	0.003	4.3
8	10	50	1.0	C	8	0.8	0.04	0.1	1.1e2
9	10	30	1.0	C	40	0.1	1.6e−2	5e−4	1.4
10	10	70	1.0	C	40	1.0	0.025	7e-3	8.7
11	30	50	1.0	C	40	0.5	0.025	0.4	1.2e2
11*	30*	50	1.0	C	40	1.0	0.05	0.4	1.2e2
12	100	50	1.0	C	40	0.2	0.01	0.7	4.3e3
13	1.0	20	3.3	A	40	< 1e−5	< 5e−7	0	1.0e−3
14	1.0	20	3.3	A	8	5e−3	2e−3	0	2.6e−2
15	3.0	20	3.3	A	40	< 1e−5	< 5e−7	0	2.8e−2
16	3.0	30	3.3	A	40	0.05	8e−3	0	7.7e−2
17	3.0	20	3.3	A	8	0.04	0.01	0	0.69
18	10	20	3.3	A	40	1e−4	3e−5	0	1.0
19	30	20	3.3	A	40	0.01	3e−3	0	28
20	100	20	3.3	A	40	0.02	6e−3	0.02	1.0e−3

and at $z=200$ km for $H=8$ km. The mass of escaping target m_t and projectile m_{pr} material were determined in an analogous way.

Numerical simulations show that most of the escaping atmospheric mass is ejected from altitudes where the projectile experiences strong deceleration and disruption. After projectile deceleration this mass is concentrated in the lower part of the wake.

As expected the entry velocity strongly influences the atmospheric erosion (see runs 3, 5 and 7, 9, 10), although it does not influence the projectile disruption and deceleration.

Fig. 4 summarizes the results of our simulations in terms of a dimensionless parameter $\chi_a(\xi)$ introduced in Shuvalov (2009). Recall that

$$\xi = \frac{D^3\rho_{pr}}{H^3\rho_a}\frac{(V^2-u_{esc}^2)}{u_{esc}^2}\frac{\rho_t}{(\rho_t+\rho_{pr})}$$

is a dimension-less impact strength, and

$$\chi_a = \frac{m_a}{M}\frac{u_{esc}^2}{(V^2-u_{esc}^2)}$$

represents the normalized escaping air mass.

Fig. 4 shows that atmospheric erosion induced by crater-forming impacts (where the projectile survives the atmospheric traversal and

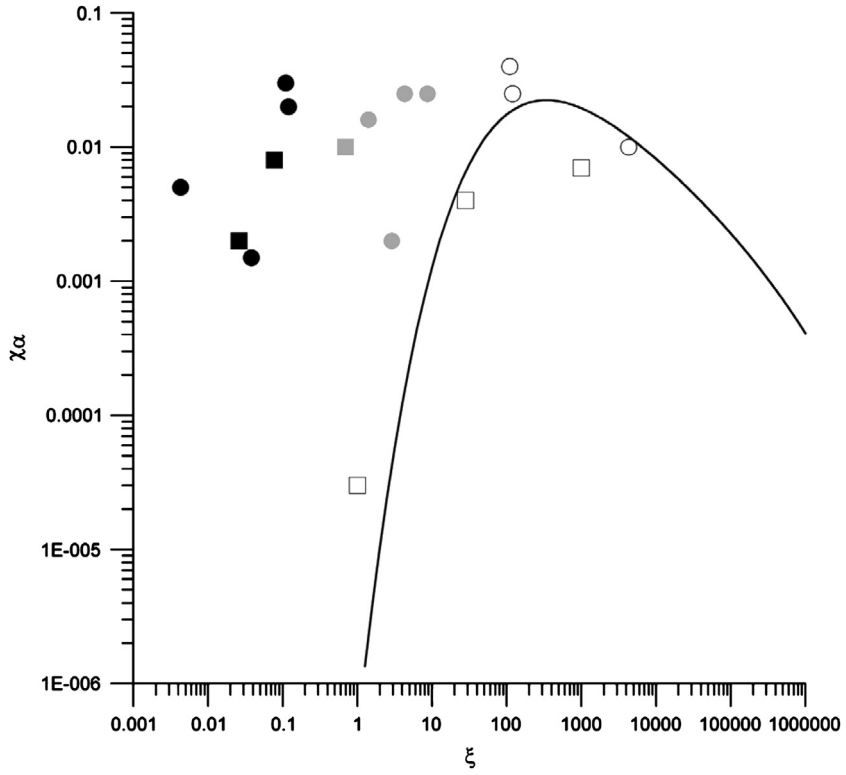

Fig. 4. Dimensionless atmospheric escape mass χ_a versus dimensionless erosional power ξ (see Section 3.2). Circles show data for cometary impacts, squares are results for asteroidal impacts. Black symbols refer to aerial bursts, gray symbols to impacts of fragmented projectiles, empty symbols to normal crater forming impacts. Escape velocity is 11.2 km/s, gray circles show data for escape velocity of 5 km/s. Black line corresponds to the approximation (Shuvalov, 2009) for crater forming impacts.

strikes the surface at hypervelocity) can be parameterized by a polynomial approximation as suggested by Shuvalov (2009):

$$\lg \chi_a = -6.375 + 5.239(\lg \xi) - 2.121(\lg \xi)^2 + 0.397(\lg \xi)^3 - 0.037(\lg \xi)^4 + 0.0013(\lg \xi)^5 \quad (4)$$

However, the atmospheric erosion induced by impacts of fragmented projectiles (runs 4, 7, 9, 10, 17) and particularly by aerial bursts (runs 1, 2, 3, 5, 6, 13, 14, 15, 16) appears to be considerably higher than predicted by Eq. (4). We regard impacts as aerial bursts if $H_{1/2} > 0$ (projectile velocity is halved before striking the ground) and refer to impacts of fragmented projectiles if $H_{fr} > 0$. Comets with diameters of 1–3 km impacting the Earth' atmosphere at 50 km/s could eject a mass of atmospheric gas as large as 0.1–0.8 M. A decrease of the entry velocity to 30 km/s (run 5) results in a much smaller amount of erosion (a few percents only), however it still remains much larger than what has been predicted for crater-forming impacts of the same dimensionless strength ξ, according to Eq. (4). Even airbursts produced by stony projectiles result in larger amounts of erosion than predicted by the approximating curve (Fig. 4 and Eq. (4)). However, the amount of erosion produced by stony projectiles of the given size (1–3 km) remains too small ($m_a/M < 1e\text{-}5$) to contribute to atmospheric evolution substantially. An increase of the entry velocity up to 30 km/s significantly increases the amount of erosion produced by asteroidal impacts (see run 16).

Numerical simulations with different equations of state for air (tabular EOS and ideal gas) show that the chemical composition of atmospheric gas only slightly influences the process of atmospheric entry (compare runs 3 and 3* in Table 1). The erosion efficiency changes within a factor of 2 (cf. runs 11 and 11* in Table 2). A ratio of specific heats $\gamma = 1.4$ was used in run 11*. We also tried smaller values of γ correspond-ding to higher temperatures or CO_2, the resulting erosion efficiency falls in the range between runs 11 and 11*.

The effect of atmospheric scale height is more complicated and depends on projectile size. On one hand a lower temperature and, consequently, smaller atmospheric scale height should result in larger upward pressure gradients within the wake, larger air acceleration and erosion. A comparison between cases 1 and 2 or 13 and 14 confirms this idea. On the other hand the temperature and atmospheric scale height strongly affect the process of atmospheric entry and type of impact (aerial bursts or crater-forming impacts). Comets of 3 km diameter produce aerial bursts for $H = 40$ km (case 3) and surface impacts (of fragmented projectile) for $H = 8$ km (case 4). In this example we find an increase of the amount of erosion for $H = 40$ km because aerial bursts are more effective (from the viewpoint of erosion). 10 km diameter comets produce approximately the same erosion: $m_a/M = 0.5$ for $H = 40$ km (case 7, impact of fragmented projectile) and $m_a/M = 0.8$ for $H = 8$ km (case 8, a crater-forming impact).

We have also extended our simulations to larger projectile sizes, up to $D = 100$ km. At the impact of a 100-km-diameter cometary object the escaping air mass is well predicted by the approximating curve (Fig. 4). At the impact of a 100-km-diameter asteroid the lost atmospheric mass is considerably smaller (by a factor of 3–4) than predicted by this approximation.

The relative mass of escaping projectile material for crater-forming impacts correlates well with the approximation by Shuvalov (2009). The mass of escaping projectile material in aerial bursts is rather small ($m_{pr}/M \ll 1$) and can be neglected for the evaluation of atmospheric loss processes. The same is true for the escape of target material.

4. Discussions and conclusions

In previous studies (e.g. Shuvalov, 2009) quantified atmospheric erosion by large crater-forming impacts that do not

experience fragmentation and deceleration during the traversal of Earth's atmosphere. In this paper we focus on atmospheric erosion due to smaller bodies leading to aerial bursts or surface impact of highly fragmented projectiles. Our numerical simulations show that aerial bursts produced by high-velocity (>30 km/s) comets and asteroids could result in the escape of air masses comparable with that of the impactor. Aerial bursts produced by comets and asteroids with velocities of 15–20 km/s are much less efficient in terms of atmospheric erosion and negligible for assessing the effect of impact on the evolution of atmospheres.

The results presented in Fig. 4 show that atmospheric erosion as a consequence of aerial bursts and impacts of fragmented projectiles cannot be approximated by the parameterization in Eq. (4) and may not be described by any $\chi_a(\xi)$ function as suggested by Shuvalov (2009). The two different mechanisms of erosion (aerial bursts and crater forming impacts) call for separate parameterizations to approximate the loss of atmosphere due to hypervelocity impact. First of all we need to determine the transition between different impact regimes. If we assume an exponential atmosphere we can rewrite the expression (2) in the form (Svetsov et al., 1995)

$$\delta_h = 2H\sqrt{\frac{\rho_h}{\rho_{pr}}} = 2H\sqrt{\frac{\rho_0}{\rho_{pr}}}\exp\left(-\frac{h}{2H}\right), \tag{5}$$

where δ_h and ρ_h are the deformation and atmospheric density at an altitude h, ρ_0 is the surface value of ρ. This equation can be rewritten to find an altitude h where the deformation reaches a specific value

$$h = -2H\ln\left(\frac{\beta D}{2H}\sqrt{\frac{\rho_{pr}}{\rho_0}}\right). \tag{6}$$

Here $\beta = \delta_h/D$ is the deformation measured in projectile diameters. Note that Eq. (6) is only a first order approximation as the atmospheric density does not precisely decrease exponentially with altitude as assumed in Eq. (5). Nevertheless, Eq. (6) suggests an approximation of H_{fr} and $H_{1/2}$ by

$$H_{1/2} = -A_{1/2}H\ln\left(\frac{B_{1/2}D}{2H}\sqrt{\frac{\rho_{pr}}{\rho_0}}\right) \tag{7}$$

$$H_{fr} = -A_{fr}H\ln\left(\frac{B_{fr}D}{2H}\sqrt{\frac{\rho_{pr}}{\rho_0}}\right) \tag{8}$$

Assuming $A_{fr}=1.4$, $B_{fr}=3.5$, $A_{1/2}=1.4$, $B_{1/2}=5.5$ yields values for H_{fr} and $H_{1/2}$ as shown in Table 3 that correlate well with the results of numerical simulations.

The atmospheric erosion induced by aerial bursts can be approximated by

$$\left(\frac{m_a}{M}\right)_{ab} = 5.5\times10^{-3}(V-V_*)^2\sqrt{\rho_{pr}}\left(\frac{D}{H}\right) \tag{9}$$

where V_* is the minimum entry velocity resulting in atmospheric erosion; here ρ_{pr} is in g/cm^3 and V in km/s. The value of V_* should decrease as the atmospheric scale height decreases. As mentioned above, this is the case because smaller atmospheric scale height results in bigger upward pressure gradients within the wake and, therefore, causes enhanced upwards acceleration of air

$$V_* = 15+0.2H \tag{10}$$

The results obtained with Eqs. (9) and (10) are given in Table 3 (runs 1, 2, 3, 5, 6, 13, 14, 15, 16) and correlate well with the results of numerical modeling. We consider that Eqs. (9) and (10) give a good approximation for dense (about 100 bar) atmospheres. We did not test (9–10) for rarified atmospheres. However, in current atmospheres the aerial bursts occur only during impacts of rather small (about 100 m) bodies which are not representative for the atmospheric effect of the total flux of impactors.

Most challenging is to find a parameterization for atmospheric loss due to impacts of fragmented projectiles. Here we suggest a smooth transition between the parameterization for crater-forming impacts (Eq. (4)) and that for aerial bursts (Eqs. (9) and (10)):

$$\ln\left(\frac{m_a}{M}\right)_{fr} = \ln\left(\frac{m_a}{M}\right)_{cr} + \left(\ln\left(\frac{m_a}{M}\right)_{ab} - \ln\left(\frac{m_a}{M}\right)_{cr}\right)\frac{H_{fr}}{(H_{fr}-H_{1/2})} \tag{11}$$

As a result the following algorithm can be used for evaluation of atmospheric erosion. The values for H_{fr} and $H_{1/2}$ are determined from Eqs. (7) and (8); note that both values could be negative. If $H_{fr}<0$ the impact is considered to be crater-forming and Eq. (4) is used to calculate the amount of erosion. If $H_{1/2}>0$ the impact is regarded as aerial burst and Eqs. (9) and (10) are used to work out how much atmosphere is eroded. Estimates for impacts of fragmented projectiles ($H_{1/2}<0$, $H_{fr}>0$) are obtained from (11). The values obtained with this algorithm are listed in Table 3, column 7. For part of cases (9 and 17 in Table 3) the results of our numerical simulations considerably deviate from the parameterization we suggested to estimate the atmospheric loss (Eqs. (7)–(10)). We think these differences occur because relatively small errors in estimating $H_{1/2}$ strongly influence the value of m_a/M. We believe that this discrepancy does not strongly change the result when averaging over projectile sizes.

Table 3
Comparison of results of numerical simulations and simple approximations,depending on impact type. *N* is the number of run, letters A and F distinguish type of impact (A — aerial burst, F — impact of fragmented projectile), *D* the denotes projectile diameter, *V* the entry velocity, C/A is the impactor type (comet or asteroid), and *H* the atmospheric scale height. Further m_a/M is the escaping atmospheric mass vs. projectile mass, H_{fr} the altitude of projectile fragmentation, $H_{1/2}$ the altitude where projectile velocity is halved.

N	*D*, km	*V*, km/s	C/A	*H*, km	m_a/M	m_a/M estimate	$H_{1/2}$, km	$H_{1/2}$, km estimate	H_{fr}, km	H_{fr}, km estimate
1 A	1.0	50	C	40	0.1	0.1	123	125	150	149
2 A	1.0	50	C	8	0.6	0.5	17	12	24	17
3 A	3.0	50	C	40	0.4	0.3	65	63	100	88
4 F	3.0	50	C	8	1.2	1	–	−0.3	4	5
5 A	3.0	30	C	40	0.03	0.02	60	63	97	88
6 A	3.0	20	C	40	<1e−5	0	67	63	98	88
7 F	10	50	C	40	0.5	0.4	–	−4	10	21
9 F	10	30	C	40	0.1	0.02	–	−4	20	21
10 F	10	70	C	40	1.0	1.4	–	−4	15	21
13 A	1.0	20	A	40	<1e−5	0	88	91	125	116
14 A	1.0	20	A	8	5e−3	1e−2	12	6	18	11
15 A	3.0	20	A	40	<1e−5	0	35	30	60	55
16 A	3.0	30	A	40	0.05	0.06	40	30	63	55
17 F	3.0	20	A	8	0.004	1e-4	–	−7	4	2

The dependence of fractional (in units of projectile mass) escaping mass on impactor size has two maxima: a first one for crater-forming impacts (where $\xi=200$–300) and a second one for aerial bursts. The actual (not fractional) mass monotonously increases with impactor scale.

Besides atmospheric loss processes aerial bursts are also interesting from the viewpoint of the maximum pressure experienced by the projectile during impact. The projectiles decelerate at some altitude (depending on size, atmospheric mass and temperature) where aerodynamic loading is smaller than near the surface. Obviously in aerial bursts the projectile material is less compressed and pressures are smaller than in the crater-forming impacts. Organic compounds have more chances to survive aerial bursts than surface impacts. This problem needs to be investigated in more detail and is beyond the scope of this paper.

In the modern relatively rarefied Earth atmosphere aerial bursts are produced by small (<100–300 m) comets. The existence and abundance of such small comets are still being questioned and small comets are not considered to be a major type of impactors in the early Earth's history (Kuzmitcheva and Ivanov, 2008). However, in the dense primary atmospheres larger projectiles can be decelerated and fragmented when passing the gaseous envelope of planets. Our simulations show that comets with sizes from 1 to 10 km could strongly influence the evolution of atmospheres 100–200 times more massive than the modern one.

Acknowledgments

This research has been supported by the Helmholtz Association through the research alliance “Planetary Evolution and Life”.

References

Cameron, A.G.W., 1983. Origin of the atmospheres of the terrestrial planets. Icarus 56 (2), 195–201.

de Niem, D., Kührt, E., Morbidelli, A., Motschmann, U., 2012. Atmospheric erosion and replenishment induced by impacts upon the Earth and Mars during a heavy bombardment. Icarus 221, 495–507.

Grigorian, S.S., 1979. Motion and disintegration of meteorites in planetary atmospheres. Cosmic Research 17 (6), 875–893. (On the Motion and Disruption of Meteorites in Planetary Atmospheres, Kosm. Issled., 17, 724–740).

Hills, J.G., Goda, M.P., 1993. The fragmentation of small asteroids in the atmosphere. Astronomical Journal 105, 1114–1144.

Kuzmitcheva, M., Ivanov, B.A., 2008. Cometary hazards. In: Adushkin, V.V., Nemchinov, I.V. (Eds.), Catastrophic Events Caused by Cosmic Objects. Hardcover, Springer Publishing Co., Dordrecht, the Netherlands, pp. 117–130.

Kuznetsov, N.M., 1965. Thermodynamic Functions and Shock Adiabats for Air at High Temperatures. Mashinostroyenie, Moscow p. 464. (in Russian).

Nemchinov, I.V., Shuvalov, V.V., 2003. Geophysical consequences of impacts of small asteroids and comets, Geofizicheskie protsessy v nizhnikh i verkhnikh obolochkakh (Geophysical Processes in Upper and Lower Shells of the Earth). IDG RAN, Moscow, pp. 36–47.

Newman, W.I., Symbalisty, E.M.D., Ahrens, T.J., Jones, E.M., 1999. Impact erosion of planetary atmospheres: some surprising results. Icarus 138, 224–240.

Pierazzo, E., Vickery, A.M., Melosh, H.J., 1997. A re-evaluation of impact melt production. Icarus 127, 408–423.

Shuvalov, V.V., 2009. Atmospheric erosion induced by oblique impacts. Meteoritics and Planetary Science 44, 1095–1105.

Shuvalov, V.V., Artemieva, N.A., 2002. Atmospheric erosion and radiation impulse induced by impacts. In: Koeberl, C., MacLeod, K.G. (Eds.), In Catastrophic Events and Mass Extinctions: Impacts and Beyond. Geological Society of America, Boulder, pp. 695–704. (GSA Special Paper 356).

Shuvalov, V.V., Trubetskaya, I.A., 2007. Aerial bursts in the terrestrial atmosphere. Solar System Research 41 (3), 220–230.

Shuvalov, V.V., Artem'eva, N.A., Kosarev, I.B., 1999. 3D hydrodynamic code SOVA for multimaterial flows, application to Shoemaker-Levy 9 comet impact problem. International Journal of Impact Engineering 23, 847–858.

Svetsov, V.V., 2007. Atmospheric erosion and replenishment induced by impacts of cosmic bodies upon the Earth and Mars. Solar System Research 41 (1), 28–41.

Svetsov, V.V., Nemtchinov, I.V., Teterev, A.V., 1995. Disintegration of large meteoroids in Earth's atmosphere: theoretical models. Icarus 116, 131–153.

Thompson, S.L., Lauson, H.S., 1972. Improvements in the Chart D Radiation-Hydrodynamic CODE III: Revised Analytic Equations of State, Report SC-RR-71 0714. Sandia National Laboratory, Albuquerque.

Tillotson, J.H., 1962. Metallic Equations of State for Hypervelocity Impact. General Atomic Report GA-3216.

Tsvetkov, V.I., Skripnik, A.Y., 1991. Atmospheric fragmentation of meteorites according to the strength theory. Solar System Research 25, 273–279.

Vasilyev, N.A., 1998. The Tunguska meteorite problem today. Planetary and Space Science 46, 129–150.

Vickery, A.M., Melosh, H.J., 1990. Atmospheric erosion and impactor retention in large impacts with application to mass extinctions. In: Sharpton, V.L., Ward, P.D. (Eds.), Global Catastrophes in Earth history. Geological Society of America, Boulder, pp. 289–300. (GSA Special Paper 247).

Wasson, J.T., Boslough, M.B.E., 2000. Large aerial bursts: an important class of terrestrial accretionary events, Catastrophic Events and Mass Extinctions: Impact and Beyond. Lunar and Planetary Institute, Houston, pp. 239–240. (LPI Contribution No. 1053).

Zahnle, K.J.N., Arndt, N., Cockell, C., Halliday, A., Nisbet, E., Selsis, F., Sleep, N.H., 2007. Emergence of a habitable planet. Space Science Reviews 129, 35–78.